Astron. Astrophys. 233, 141–152 (1990)

ASTRONOMY AND ASTROPHYSICS

The n^{th} order moment W_n^D of a resonance doublet P Cygni line profile

J. Surdej⋆ **and D. Hutsemékers**⋆⋆,⋆⋆⋆

Institut d'Astrophysique, Université de Liège, Avenue de Cointe 5, B-4200 Cointe-Ougrée, Belgium

Received November 17, 1988; accepted December 21, 1989

Abstract. In the framework of the Sobolev approximation, we have developed in the present paper the theory of the n^{th} order moment $W_n^D \propto \int (E(\lambda)/E_c - 1)(\lambda - \lambda_D)^n d\lambda$ of a P Cygni line profile $E(\lambda)/E_c$ due to a resonance doublet line transition with an effective wavelength λ_D. We show that in the optically thick approximation, the asymptotic value $W_n^{D,t}$ is entirely dependent on both the doublet separation Δ and the type of the velocity field $v(r)$ characterizing the expanding atmosphere. As expected, the most useful P Cygni profiles appear to be those which are unsaturated. From the observed moments W_n^D of such profiles, it is possible to derive the value of the parameters $W_n^{D,0}$, irrespective of the types of the velocity and opacity $\tau_D^r(X')$ distributions and of the doublet separation Δ. The parameters $W_n^{D,0}$ ($n = 1$, 2 and 3) are simply related to astrophysical quantities of general interest. For instance, $W_1^{D,0}$ is directly proportional to $\dot{M}\bar{n}^{(1)}$(level), where $\dot{M}$ is the mass-loss rate and $\bar{n}^{(1)}$(level) the average fractional abundance of the relevant ion. Adopting eighteen possible combinations of realistic velocity and opacity distributions, we have carried out extensive numerical calculations of W_n^D. Although we intend to publish elsewhere the bulk of these data ($\simeq$17280 pairs of calculated moments), several diagrams of astrophysical interest are presented here. For instance, we explain how to use the very compact "$\log_{10}(W_n^D/W_n^{D,t}) - \log_{10}(W_n^{D,0}/W_n^{D,t})$" diagrams in order to infer the value of $W_n^{D,0}$ from the measurement of W_n^D. We also describe how to determine the types of the velocity and opacity distributions from the location of the observed moments W_n^D in theoretical "$\log_{10}(W_1^D) - \log_{10}(-W_0^D)$" and "$\log_{10}(W_3) - \log_{10}(W_1^D)$" diagrams. Finally, we discuss the limits and the possible applications of this theory to existing sets of observations.

Key words: radiative transfer – Sobolev approximation – mass-loss – P Cygni line profiles – moments W_n

1. Introduction

A very convenient way to retrieve the physical information contained in an observed P Cygni line profile $E(\lambda)/E_c$ due to a *single* resonance line transition $1 \rightleftharpoons 2$ is to make use of its calculated moments $W_n^s \propto \int (E(\lambda)/E_c - 1)|\lambda - \lambda_{12}|^n \,\mathrm{sign}\,(\lambda - \lambda_{12})\, d\lambda$ (see Surdej, 1985 and references therein). As a first application, we have suggested to represent in theoretical "$\log_{10}(W_n^s) - \log_{10}(W_{n'}^s)$" diagrams ($n \neq n'$) the measured values of the moments W_n^s ($n = 0$, 1, 2 and 3) in order to infer the types of opacity ($\tau_{12}^r(v)$) and velocity ($v(r)$) distributions characterizing the rapidly expanding atmosphere in which the observed line profile is formed. We have also shown that the moments W_0^s, W_1^s, W_2^s and W_3^s, measured for an unsaturated P Cygni line profile, are directly related to the column density N_1, to the fractional mass-loss rate $\dot{M}\bar{n}^{(1)}$(level) $-\bar{n}^{(1)}$(level) representing the average fractional abundance of the considered ion –, to the column momentum and to (twice) the column kinetic energy, respectively, of the relevant species in the flow. The relation between W_1^s and $\dot{M}\bar{n}^{(1)}$(level) has been generalized to the cases of *resonance doublet* (Surdej, 1982) and *subordinate* (Hutsemékers and Surdej, 1987) line transitions. However, the other relations ($n = 0$, 2, 3, etc.) as well as the use of the "$\log_{10}(W_n^s) - \log_{10}(W_{n'}^s)$" diagrams are not directly applicable to the analysis of resonance doublet profiles. There are at least two reasons for this: (i) the expression of the line profile function $E(\lambda)/E_c$ characterizing a doublet line transition appears to be more complex than the one describing a single line transition, (ii) if λ_D denotes the central wavelength of a resonance doublet, the above expression of the moment has to be replaced by $W_n^D \propto \int (E(\lambda)/E_c - 1)(\lambda - \lambda_D)^n d\lambda$ such that physically tractable relations may still be established in the optically thin approximation.

Because most of P Cygni profiles observed in the UV spectra of early-type stars, planetary nebula nuclei as well as in the optical spectra of high redshift BAL quasars are due to resonance doublet line transitions, there is an obvious interest to develop

Send offprint requests to: J. Surdej

⋆ Chercheur qualifié au Fonds National de la Recherche Scientifique (Belgium)

⋆⋆ Aspirant au Fonds National de la Recherche Scientifique (Belgium)

⋆⋆⋆ Present address: European Southern Observatory, La Silla, Casilla 19001, Santiago 19, Chile

the theory of the n^{th} order moment W_n^D. The present paper constitutes a first step in that direction.

In Sect. 2, we first establish the expression of W_n^D assuming that there is no radiative coupling between the two single resonance line transitions of the doublet. The complex radiative interactions between line photons emitted in the transitions $1 \rightleftharpoons 2$ and $1 \rightleftharpoons 3$ and atoms located throughout the expanding atmosphere are subsequently taken into account when deriving the general expression of W_n^D in Sect. 3. Asymptotic values of W_n^D in the optically thin and optically thick approximations are also derived there. Section 4 deals with numerical applications and a few diagrams of astrophysical interest are presented and described in Sect. 5. The physical representation of selected parameters derived from the observed moments of resonance doublet P Cygni profiles is given in Sect. 6 and general conclusions form the last Section.

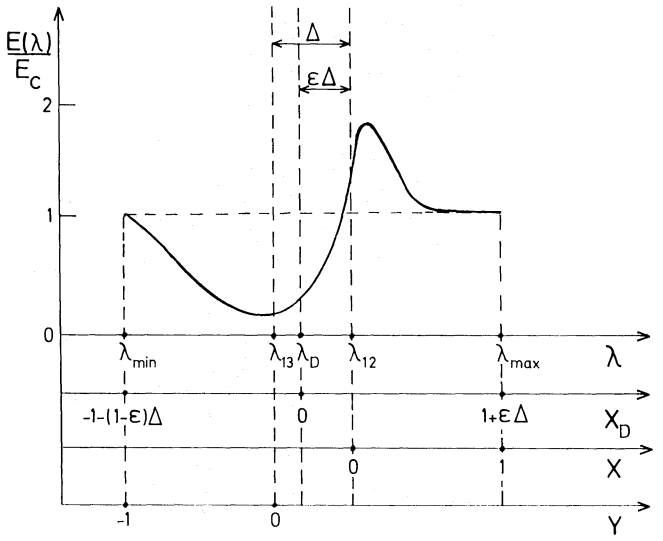

Fig. 1. Schematic example of a resonance doublet P Cygni line profile $E(\lambda)/E_c$ plotted versus the observed wavelength λ and the dimensionless frequencies X_D, X and Y (see text). We have here assumed that $\Delta = 1/2$ and $\varepsilon = 2/3$

2. Approximation of a resonance doublet by two independent line transitions

Adopting the following expression for the n^{th} order moment W_n^D of a resonance doublet P Cygni line profile (the subscript "D" standing for "doublet")

$$W_n^D = \left(\frac{c}{\lambda_D v_\infty}\right)^{n+1} \int \left(\frac{E(\lambda)}{E_c} - 1\right)(\lambda - \lambda_D)^n \, d\lambda , \tag{1}$$

where the effective wavelength of the doublet is

$$\lambda_D = (1 - \varepsilon)\lambda_{12} + \varepsilon\lambda_{13} , \tag{2}$$

with

$$\varepsilon = f_{13}/(f_{12} + f_{13}) , \tag{3}$$

λ_{12}, f_{12} (resp. λ_{13}, f_{13}) denoting the central wavelength and oscillator strength of the line transition $1 \rightleftharpoons 2$ (resp. $1 \rightleftharpoons 3$) and v_∞ the maximal radial velocity $v(r)$ of the flow, and making use of the dimensionless frequency

$$X_D = \left(\frac{\lambda - \lambda_D}{\lambda_D}\right)\frac{c}{v_\infty} , \tag{4}$$

it is straightforward to reduce Eq. (1) to

$$W_n^D = \int_{-1-(1-\varepsilon)\Delta}^{1+\varepsilon\Delta} \left(\frac{E(X_D)}{E_c} - 1\right) X_D^n \, dX_D . \tag{5}$$

It is also very convenient to define (cf. Eq. (4) and Fig. 1) the dimensionless frequencies X and Y associated with λ_{12} and λ_{13}, such that

$$X = X_D - \varepsilon\Delta \tag{6}$$

and

$$Y = X_D + (1 - \varepsilon)\Delta , \tag{7}$$

with

$$\Delta = \Delta v_{23}/v_\infty , \tag{8}$$

Δv_{23} being the Doppler velocity separation between the two line transitions of the resonance doublet (cf. Surdej, 1980, hereafter referred to as Paper I; see also Lamers et al., 1987). If one may assume that the composite line profile $E(X_D)/E_c$ results from the mere superposition of the two line profile functions $E_{12}(X)/E_c$ and $E_{13}(Y)/E_c$, each being independently formed from one another, we obtain the interesting relation

$$W_n^D = \int_{-1}^{+1} \left(\frac{E_{12}(X)}{E_c} - 1\right)(X + \varepsilon\Delta)^n \, dX + \int_{-1}^{+1} \left(\frac{E_{13}(Y)}{E_c} - 1\right)(Y - (1 - \varepsilon)\Delta)^n \, dY . \tag{9}$$

This result is rigorously exact in only two cases: (i) when the expanding atmosphere is optically thin to the spectral line radiation, and (ii) for values of the doublet separation $\Delta \geq 2$.

Defining the moments W_n^{12} and W_n^{13} (the subscripts "12" and "13" referring to the single line transitions $1 \rightleftharpoons 2$ and $1 \rightleftharpoons 3$, respectively) by means of Eq. (5), where we have replaced X_D by X and Y, respectively, we can express Eq. (9) as follows:

$$\begin{aligned}
W_0^D &= W_0^{12} + W_0^{13} , \\
W_1^D &= W_1^{12} + W_1^{13} + \varepsilon\Delta W_0^{12} - (1 - \varepsilon)\Delta W_0^{13} , \\
W_2^D &= W_2^{12} + W_2^{13} + 2\varepsilon\Delta W_1^{12} - 2(1 - \varepsilon)\Delta W_1^{13} \\
&\quad + \varepsilon^2\Delta^2 W_0^{12} + (1 - \varepsilon)^2\Delta^2 W_0^{13} , \\
W_3^D &= W_3^{12} + W_3^{13} + 3\varepsilon\Delta W_2^{12} - 3(1 - \varepsilon)\Delta W_2^{13} + 3\varepsilon^2\Delta^2 W_1^{12} \\
&\quad + 3(1 - \varepsilon)^2\Delta^2 W_1^{13} + \varepsilon^3\Delta^3 W_0^{12} - (1 - \varepsilon)^3\Delta^3 W_0^{13} ,
\end{aligned} \tag{10}$$

i.e. the moments W_n^D ($n = 0, 1, 2$ and 3) appear as straightforward linear combinations of the moments $W_{n'}^{12}$ and $W_{n'}^{13}$ ($n' \leq n$) of each of the single line transitions forming the resonance doublet. It is interesting to consider now the two usual asymptotic regimes: the optically thin and optically thick approximations.

2.1. The optically thin approximation

For the case of optically thin lines, it is easy to show (see Appendix A) that the moment W_n^{ij}, associated with a single resonance

transition $i \rightleftharpoons j$, is directly proportional to the oscillator strength f_{ij}. We can therefore write the equality

$$\varepsilon W_n^{12} = (1-\varepsilon) W_n^{13}, \tag{11}$$

such that relation (10) reduces now to (the subscript "o" referring to the optically thin case):

$$\begin{aligned} W_0^{D,0} &= (W_0^{12} + W_0^{13}), \\ W_1^{D,0} &= (W_1^{12} + W_1^{13}), \\ W_2^{D,0} &= (W_2^{12} + W_2^{13}) + \Delta^2 \varepsilon(1-\varepsilon)(W_0^{12} + W_0^{13}), \\ W_3^{D,0} &= (W_3^{12} + W_3^{13}) + 3\Delta^2 \varepsilon(1-\varepsilon)(W_1^{12} + W_1^{13}) \\ &\quad + \Delta^3 \varepsilon(1-\varepsilon)(2\varepsilon - 1)(W_0^{12} + W_0^{13}). \end{aligned} \tag{12}$$

Replacing the values of the moment $W_n^{12} + W_n^{13}$ in Eq. (12) by those given for an optically thin, single resonance line having an equivalent oscillator strength $f_D = f_{12} + f_{13}$ and a central wavelength λ_D (see Surdej, 1982, hereafter referred to as Paper II), it will be easy and useful in Sect. 3.3 to compare the above results with those derived from the rigorous expression of W_n^D.

2.2. *The optically thick approximation*

Equation (10) can also be conveniently used to calculate asymptotic values of W_n^D when the atmosphere gets optically thick and $\Delta \to 2$. Assuming that $\tau_{12} \gg 1$, $\tau_{13} \gg 1$ (see Paper II), we have

$$W_n^{12} = W_n^{13} = W_n^{\text{thick}} = W_n^t, \tag{13}$$

such that Eq. (10) now transforms into (the subscript "t" referring to the optically thick case)

$$\begin{aligned} W_0^{D,t} &= 2W_0^t, \\ W_1^{D,t} &= 2W_1^t + (2\varepsilon - 1)\Delta W_0^t, \\ W_2^{D,t} &= 2W_2^t + 2(2\varepsilon - 1)\Delta W_1^t + \Delta^2(2\varepsilon^2 - 2\varepsilon + 1) W_0^t, \\ W_3^{D,t} &= 2W_3^t + 3(2\varepsilon - 1)\Delta W_2^t + 3\Delta^2(2\varepsilon^2 - 2\varepsilon + 1) W_1^t \\ &\quad + (\varepsilon^3 - (1-\varepsilon)^3)\Delta^3 W_0^t, \end{aligned} \tag{14}$$

i.e. the moments $W_n^{D,t}$ ($n = 0$, 1, 2 and 3) are simple linear combinations of the moments $W_{n'}^t$ ($n' \leq n$) of an optically thick, single line transition which central wavelength and oscillator strength are not necessarily specified. Replacing in Eq. (14) the values of W_n^t by those calculated for the case of a single resonance line profile that is formed in an optically thick atmosphere (see Paper II), one easily derives the asymptotic values of W_n^D. Since the former ones essentially depend on the velocity distribution characterizing the outflow, we have reported in Table 2 values of W_n^t and $W_n^{D,t}$ for the three velocity fields listed in Table 1. We have also adopted $X_{\min} = -0.01$, $\varepsilon = 2/3$ and $\Delta = 1.8$. These results will be compared in Section 3.4 with self-consistent calculations of W_n^D.

3. The general case

Considering a three-level atom model, the transfer of spectral line radiation in a rapidly expanding envelope is complicated by the fact that photons emitted at a point R in the transition $3 \rightarrow 1$ may interact with atoms at distant points R′, via the line transition $1 \rightleftharpoons 2$. We refer the reader to Paper I for a comprehensive study of these distant interactions between atoms and line photons. In the framework of the Sobolev approximation, we establish hereafter the general expression of the resonance doublet profile formed in an atmosphere that is rapidly expanding around a central stellar core having a finite radius R_*.

Table 1. Adopted velocity and opacity distributions for calculating the moments W_n^D of resonance doublet P Cygni line profiles

(A)	$X' = -X_{\min} + (1 + X_{\min})(1 - 1/\sqrt{L})$
(B)	$X' = -X_{\min} + (1 + X_{\min})(1 - 1/L)$
(C)	$X' = \sqrt{1 - (1 - X_{\min}^2)/L}$
(α)	$\tau'(X') = d(1/L)/X'\,dX'$
(β)	$\tau'(X') = 1 - X'$
(γ)	$\tau'(X') = 1$
(δ)	$\tau'(X') = (1 - X')^{1/2}$
(ε)	$\tau'(X') = (1 - X')^2$
(η)	$\tau'(X') = 1/X'$

3.1. *Expression of the resonance doublet profile $E(X_D)/E_c$*

The general expression $E(X_D)/E_c$ of a resonance doublet P Cygni profile formed in a spherically symmetric atmosphere may be written as (see Eq. (II.42) for the restricted case of a point-like star)

$$\frac{E(X_D)}{E_c} = \frac{E_{12}(X = X_D - \varepsilon\Delta)}{E_c} + \frac{E_{13}(Y = X_D + (1-\varepsilon)\Delta)}{E_c} + \frac{E_{\text{abs}}(X_D)}{E_c}, \tag{15}$$

where the different contributions refer to the scattered line photons in the resonance transitions $1 \rightleftharpoons 2$ and $1 \rightleftharpoons 3$, as well as to the stellar photons which did not suffer any scattering. In the absence of limb darkening and assuming that the central core radiates with an intensity I_c that is constant over the frequency range $X_D \in [-1 - (1-\varepsilon)\Delta, 1 + \varepsilon\Delta]$ (see Fig. 1), one can easily derive, with the help of Eqs. (II.56), (II.67) and (II.69), the following expressions:

$$\frac{E_{12}(X)}{E_c} = \begin{cases} \displaystyle\int_{\max(|X|, -X_{\min})}^{1} P_{12}^N(X')\, P_{12}(X', X)\, \frac{dX'}{2X'}, & \text{if } X \in [-1, 0], \\ \displaystyle\int_{\max(|X^N|, -X_{\min})}^{1} P_{12}^N(X')\, P_{12}(X', X)\, \frac{dX'}{2X'}, & \text{if } X \in]0, X^0], \\ 1, & \text{if } X \in]X^0, 1], \end{cases} \tag{16}$$

Table 2. Asymptotic values of W_n^t and $W_n^{D,t}$ according to Eqs. (13) and (14) for $\varepsilon = 2/3$ and $\Delta = 1.8$

Velocity field	$\log(-W_0^t)$	$\log(W_1^t)$	$\log(-W_2^t)$	$\log(W_3^t)$
A	−1.143	−0.338	−0.636	−0.660
B	−0.914	−0.323	−0.607	−0.609
C	−0.724	−0.344	−0.609	−0.616
	$\log(-W_0^{D,t})$	$\log(W_1^{D,t})$	$\log(-W_2^{D,t})$	$\log(W_3^{D,t})$
A	−0.842	−0.058	−1.387	0.411
B	−0.613	−0.057	−0.842	0.419
C	−0.424	−0.101	−0.539	0.380

with

$$X_{\min} = -v_0/v_\infty , \tag{17}$$

v_0 being the radial velocity at the stellar surface and where the frequency X^N fulfils the condition

$$X^N = -X/(1 - 2W(L(X^N))) . \tag{18}$$

$W(L(X^N))$ stands for the geometrical dilution factor

$$W(L) = \frac{1}{2}(1 - \sqrt{1 - (1/L)^2}), \tag{19}$$

evaluated at the radial distance $r(X^N) = L(X^N)R_*$, where the reduced radial velocity

$$X' = v(r)/v_\infty \tag{20}$$

is equal to $-X^N$.
The frequency

$$X^0 = 1 - 2W(L_{\max}) \tag{21}$$

is such that for $X > X^0$, there is total occultation of the rear part of the expanding envelope contributing to the line profile at the frequency X. $L_{\max}$ denotes the size of the atmosphere in stellar radii R_* units. Reminding results (I.24)–(I.26), (II.58) and (II.64), we easily obtain the expression of the integrands in Eq. (16):

$$P^N_{12}(X') = (\beta^5_{12}(X') + J^2_{12}(X')/I_c)\tau^r_{12}(X')4L^2(X') \tag{22}$$

and

$$P_{12}(X', X) = \frac{(1 - \exp(-\tau_{12}(X', X)))}{\tau_{12}(X', X)\beta^1_{12}(X')}, \tag{23}$$

where $\tau_{12}(X', X)$ (resp. $\tau^r_{12}(X')$) represents the fictitious opacity in the transition $1 \rightleftharpoons 2$ evaluated at the distance $L(X')$ along directions making a cosine angle

$$\mu = -X/X' , \tag{24}$$

(resp. $\mu = 1$) with the radial direction. $\beta^1_{12}(X')$ denotes the usual escape probability of a line photon (cf. Eq. (I.10)). We also have

$$\beta^5_{12}(X') = \int_{\Omega = 4\pi W} \frac{1 - \exp(-\tau_{12}(X', \omega))}{\tau_{12}(X', \omega)} \exp(-\tau_{13}(X'', \omega'')) \frac{d\omega}{4\pi} \tag{25}$$

and

$$\frac{J^2_{12}(X')}{I_c} = \int_{\Omega(R, R'')} \frac{\beta^3_{13}(X'')}{\beta^1_{13}(X'')}(1 - \exp(-\tau_{13}(X'', \omega'))) \cdot \frac{(1 - \exp(-\tau_{12}(X', \omega)))}{\tau_{12}(X', \omega)} \frac{d\omega}{4\pi}, \tag{26}$$

such that $I_c\beta^5_{12}$ and J^2_{12} account for the mean intensity of the radiation field in the transition $1 \rightleftharpoons 2$ due to the diluted stellar continuum and to line photons emitted in the transition $1 \rightleftharpoons 3$ by distant atoms located at points $R''(L(X''))$ along directions ω'' (cf. Paper I). In a very similar way, we find that

$$\frac{E_{13}(Y)}{E_c} = \begin{cases} \displaystyle\int_{\max(|Y|, -X_{\min})}^{1} P^N_{13}(X')\, P_{13}(X', Y)\, \exp(-\tau'_{12}) \frac{dX'}{2X'}, & \text{if } Y \in [-1, 0], \\ \displaystyle\int_{\max(|Y^N|, -X_{\min})}^{1} P^N_{13}(X')\, P_{13}(X', Y) \exp(-\tau'_{12}) \frac{dX'}{2X'}, & \text{if } Y \in]0, X^0], \\ 1, & \text{if } Y \in]X^0, 1], \end{cases} \tag{27}$$

where the factor $\exp(-\tau'_{12})$ expresses the probability for a photon emitted in the line transition $1 \rightleftharpoons 3$ to escape the expanding atmosphere without being scattered in the line transition $1 \rightleftharpoons 2$ by atoms located at large distances from the point of emission. All quantities appearing in Eq. (27) can be defined by analogy with those in Eq. (16), with the exception of (cf. Eq. (II.64))

$$P^N_{13}(X') = \beta^3_{13}(X')\tau^r_{13}(X')4L^2(X') , \tag{28}$$

where

$$\beta^3_{13}(X') = \int_{\Omega = 4\pi W} \frac{(1 - \exp(-\tau_{13}(X', \omega)))}{\tau_{13}(X', \omega)} \frac{d\omega}{4\pi} . \tag{29}$$

Note here that if the central continuum source were point-like (i.e. $L_{\max} \gg 1$), the contribution $P^N_{13}(X')$ would reduce to $P_{13}(X') = (1 - \exp(-\tau^r_{13}(X')))$. We remind that $P_{13}(X')$ represents the probability for a stellar photon emitted with an initial frequency X' to be scattered at a distance $L(X')$ and that $P_{13}(X', Y)$ corresponds to the probability that this photon will finally escape the expanding atmosphere along a direction making a cosine angle $\mu = -Y/X'$ with the radial direction. As far as the fraction $E_{\text{abs}}(X_D)/E_c$ of unscattered stellar photons is concerned, its contribution to the resonance doublet P Cygni line profile in the frequency interval $X_D \in [-1 - (1 - \varepsilon)\Delta, \varepsilon\Delta]$ is easily derived to be

$$\frac{E_{\text{abs}}(X_D)}{E_c} = 2 \int_0^1 \exp(-\tau_{12}(X', \mu_{12})) \exp(-\tau_{13}(Y', \mu_{13}))\, \mu_*\, d\mu_* \tag{30}$$

where

$$X' = (\varepsilon\Delta - X_D)/\mu_{12} , \tag{31}$$

with $\mu_{12} = \sqrt{1 - (1 - \mu_*^2)/L^2(X')}$, if $X_D \in [-1 + \varepsilon\Delta, \varepsilon\Delta]$,

and similarly

$$Y' = -(X_D + (1 - \varepsilon)\Delta)/\mu_{13} , \tag{32}$$

with $\mu_{13} = \sqrt{1 - (1 - \mu_*^2)/L^2(Y')}$, if $X_D \in [-1 - (1 - \varepsilon)\Delta, -(1 - \varepsilon)\Delta]$, τ_{12} (resp. τ_{13}) being set equal to zero in Eq. (30) if no solution (X', μ_{12}) (resp. (Y', μ_{13})) is found. We can now make use of all previous results (Eqs. (15)–(32)) to derive the explicit form of Eq. (5).

3.2. *Expression of the moment* W^D_n

Inserting relations (15), (16), (27) and (30) in Eq. (5) and following a procedure similar to that described in Appendix B for the

particular contribution of $E_{12}(X)/E_c$, we obtain the general result

$$W_n^D = \int_{-X_{\min}}^{1} \frac{\tau_{12}^r(X')(\beta_{12}^5(X') + J_{12}^2(X')/I_c)\,4L^2(X')}{\beta_{12}^1(X')} \cdot \frac{1}{2} \int_{-(1-2W(L(X')))}^{1} (-X'\mu + \varepsilon\Delta)^n \cdot \frac{(1-\exp(-\tau_{12}(X',\mu)))}{\tau_{12}(X',\mu)} d\mu\, dX' + \int_{-X_{\min}}^{1} \frac{\tau_{13}^r(X')\,\beta_{13}^3(X')\,4L^2(X')}{\beta_{13}^1(X')} \frac{1}{2} \int_{-(1-2W(L(X')))}^{1} \cdot (-X'\mu - (1-\varepsilon)\Delta)^n \cdot \frac{(1-\exp(-\tau_{13}(X',\mu)))}{\tau_{13}(X',\mu)} \cdot \exp(-\tau_{12}')\, d\mu\, dX' + 2\int_0^1 \mu_*\, d\mu_* \int_{-\sqrt{1-(1-\mu_*^2)/L_{\max}^2}-(1-\varepsilon)\Delta}^{X_{\min}\mu_*+\varepsilon\Delta} X_D^n \cdot (\exp(-\tau_{12}(X',\mu_{12}))\exp(-\tau_{13}(Y',\mu_{13})) - 1)\, dX_D. \quad (33)$$

For values of $L_{\max} \gg 1$, the "point-like" star approximation is essentially a good one and it provides a very useful model to understand more easily the asymptotic behavior of more general solutions given by Eq. (33). We merely state the result when $R_* \to 0$ (the subscript "*" stands here for the "point-like" star approximation)

$$W_n^{D*} = \int_{-X_{\min}}^{1} \cdot \frac{(1-\exp(-\tau_{12}^r(X')))\exp(-\tau_{13}^r) + \tau_{12}^r(X')(J_{12}^2(X')/I_c)\,4L^2(X')}{\beta_{12}^1(X')} \cdot \frac{1}{2}\int_{-1}^{+1} (-X'\mu + \varepsilon\Delta)^n \frac{(1-\exp(-\tau_{12}(X',\mu)))}{\tau_{12}(X',\mu)} d\mu\, dX' + \int_{-X_{\min}}^{1} \frac{1-\exp(-\tau_{13}^r(X')))}{\beta_{13}^1(X')} \frac{1}{2}\int_{-1}^{1} (-X'\mu - (1-\varepsilon)\Delta)^n \cdot \frac{(1-\exp(-\tau_{13}(X',\mu)))}{\tau_{13}(X',\mu)} \exp(-\tau_{12}')\, d\mu\, dX' + \int_{-1-(1-\varepsilon)\Delta}^{X_{\min}+\varepsilon\Delta} X_D^n(\exp(-\tau_{12}^r(X'))\exp(-\tau_{13}^r(Y')) - 1)\, dX_D. \quad (34)$$

3.3. *The optically thin case*

3.3.1. Central core with finite dimensions

For unsaturated ($\tau_{12} < 1, \tau_{13} < 1$) resonance doublet P Cygni profiles, Eq. (33) is easily transformed into (see Appendix C)

$$W_n^{D,0} = \int_{-X_{\min}}^{1} \tau_{12}^r(X')\, W(L(X'))\, 4L^2(X') \cdot \frac{1}{2} \int_{-(1-2W(L(X')))}^{1} (-X'\mu + \varepsilon\Delta)^n\, d\mu\, dX' + \int_{-X_{\min}}^{1} \tau_{13}^r(X')\, W(L(X'))\, 4L^2(X') \cdot \frac{1}{2} \int_{-(1-2W(L(X')))}^{1} (-X'\mu + (1-\varepsilon)\Delta)^n\, d\mu\, dX' - \int_{-X_{\min}}^{1} \tau_{12}^r(X')\, 4L^2(X') \cdot \frac{1}{2} \int_{1-2W(L(X'))}^{1} (-X'\mu + \varepsilon\Delta)^n\, d\mu\, dX' - \int_{-X_{\min}}^{1} \tau_{13}^r(X')\, 4L^2(X') \cdot \frac{1}{2} \int_{1-2W(L(X'))}^{1} (-X'\mu - (1-\varepsilon)\Delta)^n\, d\mu\, dX'. \quad (35)$$

Considering the particular values of $n = 0$, 1, 2 and 3, Eq. (35) leads to the results

$$W_0^{D,0} = \int_{-X_{\min}}^{1} (\tau_{12}^r(X') + \tau_{13}^r(X'))(1 - 4L^2W)\, dX',$$

$$W_1^{D,0} = \int_{-X_{\min}}^{1} X'(\tau_{12}^r(X') + \tau_{13}^r(X'))(1 - W)\, dX',$$

$$W_2^{D,0} = \int_{-X_{\min}}^{1} X'^2(\tau_{12}^r(X') + \tau_{13}^r(X')) \cdot \frac{2}{3}(W(1 + (1-2W)^3) - 1 + (1-2W)^3)\, L^2\, dX' + \varepsilon(1-\varepsilon)\Delta^2 \int_{-X_{\min}}^{1} (\tau_{12}^r(X') + \tau_{13}^r(X'))(1 - 4L^2W)\, dX', \quad (36)$$

$$W_3^{D,0} = \int_{-X_{\min}}^{1} X'^3(\tau_{12}^r(X') + \tau_{13}^r(X'))\left(1 - \frac{1}{2L^2}\right)(1 - W)\, dX' + 3\varepsilon(1-\varepsilon)\Delta^2 \int_{-X_{\min}}^{1} X'(\tau_{12}^r(X') + \tau_{13}^r(X'))(1 - W)\, dX' + \varepsilon(2\varepsilon - 1)(1-\varepsilon)\Delta^3 \int_{-X_{\min}}^{1} (\tau_{12}^r(X') + \tau_{13}^r(X'))(1 - 4L^2W)\, dX'.$$

Referring to the asymptotic expressions established in Appendix A for the moment W_n^{ij} ($n = 0$, 1, 2 and 3) of a single resonance line transition $i \rightleftharpoons j$, we conclude that result (36) is essentially equivalent to that given in Eq. (10) provided that all W_n^{ij} have been replaced by their corresponding expression from Eq. (A.1). This agreement partly testifies about the self-consistency of the results derived in this chapter.

3.3.2. The point-like stellar core

Following a similar reasoning as that in Appendix C, expression (34) of the moment W_n^{D*}, established for the case of a point-like star, simplifies in the optically thin approximation to

$$W_n^{D*,0} = \int_{-X_{\min}}^{1} \tau_{12}^r(X') \frac{1}{2} \int_{-1}^{+1} (-X'\mu + \varepsilon\Delta)^n\, d\mu\, dX' + \int_{-X_{\min}}^{1} \tau_{13}^r(X') \frac{1}{2} \int_{-1}^{+1} (-X'\mu - (1-\varepsilon)\Delta)^n\, d\mu\, dX'$$

$$+(-1)^{n+1}\left[\int_{-X_{\min}}^{1}\tau^r_{12}(X')(X'-\varepsilon\Delta)^n\,dX'\right.$$
$$\left.+\int_{-X_{\min}}^{1}\tau^r_{13}(X')(X'+(1-\varepsilon)\Delta)^n\,dX'\right]. \quad (37)$$

For the particular values of $n = 0$, 1, 2 and 3, we obtain

$$W_0^{D*,0} = 0,$$
$$W_1^{D*,0} = \int_{-X_{\min}}^{1} X'(\tau^r_{12}(X')+\tau^r_{13}(X'))\,dX',$$
$$W_2^{D*,0} = -\frac{2}{3}\int_{-X_{\min}}^{1} X'^2(\tau^r_{12}(X')+\tau^r_{13}(X'))\,dX', \quad (38)$$
$$W_3^{D*,0} = \int_{-X_{\min}}^{1} X'^3(\tau^r_{12}(X')+\tau^r_{13}(X'))\,dX'$$
$$+3\varepsilon(1-\varepsilon)\Delta^2\int_{-X_{\min}}^{1} X'(\tau^r_{12}(X')+\tau^r_{13}(X'))\,dX'.$$

3.4. The optically thick case

If the expanding medium is optically thick to the spectral line radiation in the transitions $i \rightleftharpoons j$ ($i = 1, j = 2$ and 3), we can make in Eq. (33) the approximation $\exp(-\tau_{ij}) = 0$, provided of course that the corresponding direction of light propagation crosses a surface of possible interaction. Furthermore, expressing in Eq. (33) the fictitious opacity $\tau_{ij}(X', \mu)$ in terms of its radial component, i.e. in a spherical envelope

$$\tau_{ij}(X',\mu) = \tau^r_{ij}(X')\Big/\left[\mu^2\left(1-\frac{d\ln L}{d\ln X'}\right)+\frac{d\ln L}{d\ln X'}\right], \quad (39)$$

we directly see that the optically thick expression of W_n^D does not depend anymore on the form of the opacity distribution $\tau^r_{ij}(X')$ but that it essentially relies on the type of velocity field $v(r)$ characterizing the expanding atmosphere. Although it is not possible to reduce Eq. (33) to a simple analytic expression when $\tau_{ij} \gg 1$, we can establish such expressions for $\beta^1_{12}(X')$, $\beta^1_{13}(X')$, $\beta^3_{13}(X')$, etc. and therefore suppress one level of integration in Eq. (33). Taking into account the exact form of the geometrical loci of distant interacting points (R, R') as a function of the relative doublet separation Δ (cf. Eq. (I.14) and see Hutsemékers, 1988), we have illustrated in Figs. 2–5 the results of numerical calculations of W_n^D versus $\Delta = 0.0$, 0.2, 0.5, 0.8, 1.0, 1.2, 1.5 and 1.8 for $n = 0$, 1, 2 and 3, adopting the velocity fields A, B and C explicited in Table 1. Let us note the very good agreement between the results calculated here for $\Delta = 1.8$ and those reported in Table 2.

4. Numerical applications

By means of Eqs. (2)–(3) and since

$$f_D = f_{12} + f_{13}, \quad (40)$$

the fictitious radial opacity of a resonance doublet line transition ($\tau^r_D(X') = \tau^r_{12}(X') + \tau^r_{13}(X')$) may be expressed as (cf. Eq. (II.19))

$$\tau^r_D(X') = K\dot{M}n(\text{level})\frac{A(\text{el})}{v_\infty^2}\frac{d(1/L)}{X'dX'}, \quad (41)$$

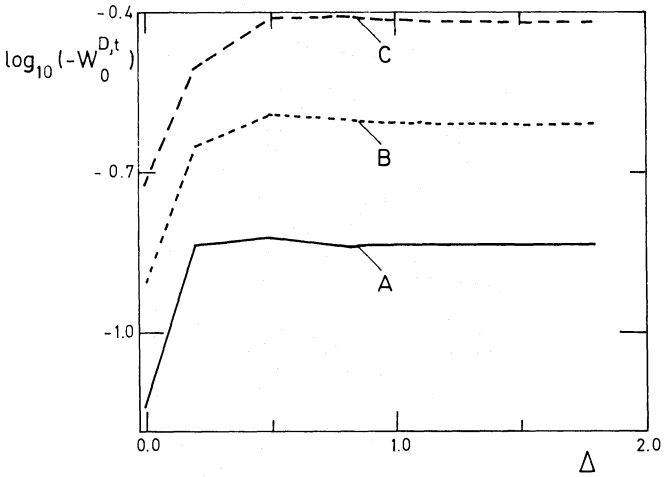

Fig. 2. $\log_{10}(-W_0^{D,t})$ values calculated from Eq. (33) as a function of the relative doublet separation $\Delta = 0.0$, 0.2, 0.5, 0.8, 1.0, 1.2, 1.5 and 1.8 assuming that $\tau_{12}, \tau_{13} \gg 1$. The three curves refer to the velocity fields A, B and C given in Table 1

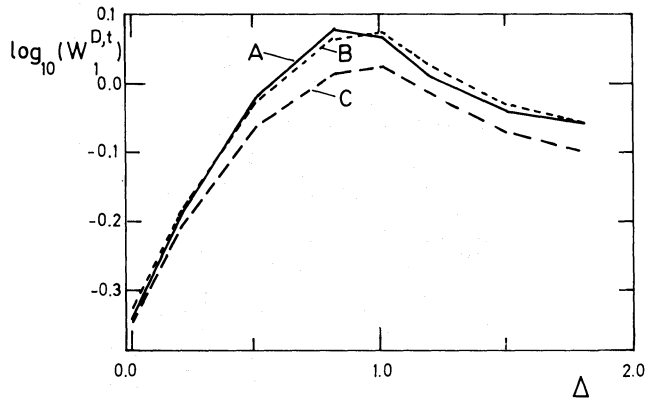

Fig. 3. Same as in Fig. 2 but for $\log_{10}(W_1^{D,t})$

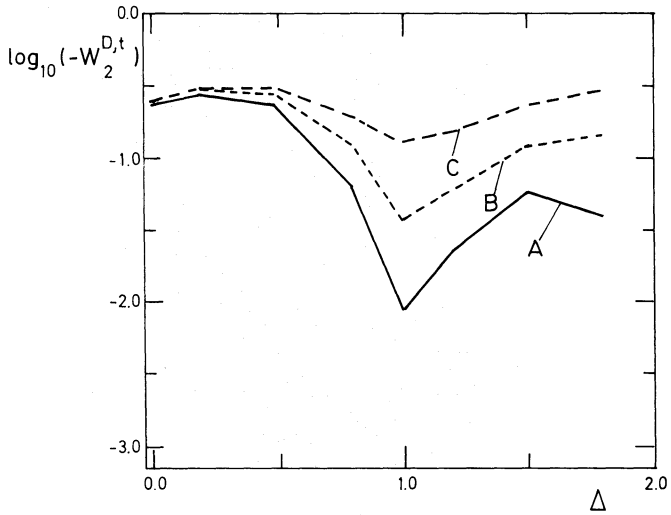

Fig. 4. Same as in Fig. 2 but for $\log_{10}(-W_2^{D,t})$

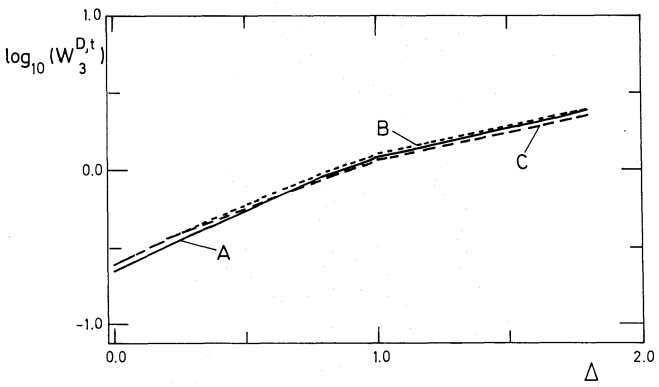

Fig. 5. Same as in Fig. 2 but for $\log_{10}(W_3^{D,t})$

with the constant

$$K = \frac{\pi e^2}{mc} f_D \lambda_D / (4\pi \bar{\mu} M_{\rm amu} R_*), \tag{42}$$

where:

A(el) represents the abundance of the relevant element,
$\bar{\mu}$ is the mean atomic weight of the nuclei and
$M_{\rm amu}$ is the unit of atomic mass; all the other symbols have their usual meaning.

Inserting Eq. (41) into expression (36) of $W_1^{D,0}$, we easily recover the linear relation existing between the first order moment of an unsaturated resonance doublet P Cygni profile and the mass-loss rate $\dot{M}$ (cf. Paper II and Surdej, 1983a, b)

$$W_1^{D,0} = K \dot{M} \bar{n}^{(1)}(\text{level}) q^{c1}(\infty) \frac{A(\text{el})}{v_\infty^2}, \tag{43}$$

where the average fractional abundance

$$\bar{n}^{(1)}(\text{level}) = \frac{\int_1^\infty n(\text{level})(1 - W)\, dL/L^2}{\int_1^\infty (1 - W)\, dL/L^2}, \tag{44}$$

and

$$q^{c1}(\infty) = -\int_1^\infty (1 - W)\, dL/L^2 = -0.89271. \tag{45}$$

If one adopts now the form of the opacity distributions given in Table 1, namely

$$\tau_D^r(X') = C^{te} \tau^r(X'), \tag{46}$$

we find out by inserting the last relation into Eq. (36) that the fictitious radial opacity $\tau_D^r(X')$ may be rewritten as

$$\tau_D^r(X') = \frac{W_1^{D,0} \tau^r(X')}{\int_{-X_{\min}}^1 \tau^r(X') X' (1 - W)\, dX'}. \tag{47}$$

It therefore appears straightforward to compute the moments W_n^D (cf. Eq. (33)) and $W_n^{D,0}$ (see Eq. (36)) as a function of the parameter $W_1^{D,0}$ for various opacity and velocity distributions as well as for different values of the doublet separation Δ. Because the moments $W_2^{D,0}$ and $W_3^{D,0}$ in Eq. (36) appear to be linear combinations (involving the doublet separation Δ) of more elementary moments alike those expressed in Eq. (A.1), it is also very convenient to define and use the following moments

$$W_2 = W_2^D - \varepsilon(1 - \varepsilon)\Delta^2 W_0^D,$$
$$W_3 = W_3^D - 3\varepsilon(1 - \varepsilon)\Delta^2 W_1^D - \varepsilon(2\varepsilon - 1)(1 - \varepsilon)\Delta^3 W_0^D. \tag{48}$$

In the optically thin approximation, the latter ones reduce to

$$W_2^0 = \int_{-X_{\min}}^1 X'^2 \tau_D^r(X') \frac{2}{3} (W(1 + (1 - 2W)^3) - 1 + (1 - 2W)^3) L^2\, dX',$$
$$W_3^0 = \int_{-X_{\min}}^1 X'^3 \tau_D^r(X') \left(1 - \frac{1}{2L^2}\right)(1 - W)\, dX', \tag{49}$$

i.e. alike $W_0^{D,0}$ and $W_1^{D,0}$ in Eq. (36), W_2^0 and W_3^0 are not dependent on the doublet separation Δ. Furthermore, we shall see in Sect. 6 that the latter moments are simply related to astrophysical quantities of general interest.

Considering the 3 velocity fields and 6 opacity distributions listed in Table 1, we have computed for the eight doublet separations $\Delta = 0.0$, 0.2, 0.5, 0.8, 1.0, 1.2, 1.5 and 1.8 the pairs of moments $(W_0^D, W_0^{D,0})$, $(W_1^D, W_1^{D,0})$, $(W_2^D, W_2^{D,0})$, (W_2, W_2^0), $(W_3^D, W_3^{D,0})$ and (W_3, W_3^0) as a function of 20 values of $\log_{10}(W_1^0)$ in the range $[-3.5, 3.5]$. We have also adopted the values $\varepsilon = 2/3$, $X_{\min} = -0.01$ and $L_{\max} = 1000$. There results a total number of $(3 \times 6 \times 8 \times 6 \times 20 =)$ 17280 pairs of calculated moments which may be represented against each other in many various ways. These data as well as more details about their calculations, accuracies, etc. will be published in a separate paper (Hutsemékers and Surdej, 1989a). Some of the most representative diagrams constructed from these data are illustrated in the next Section. We also discuss there the potential use of such diagrams in the context of astrophysical applications.

5. A few diagrams of astrophysical interest

We have illustrated in Figs. 6 and 7 typical "$\log_{10}(W_n^D) - \log_{10}(W_n^{D,0})$" curves for $n = 0$ and $n = 3$, respectively, and for two different values of the doublet separation ($\Delta = 0.2$ and 1.0).

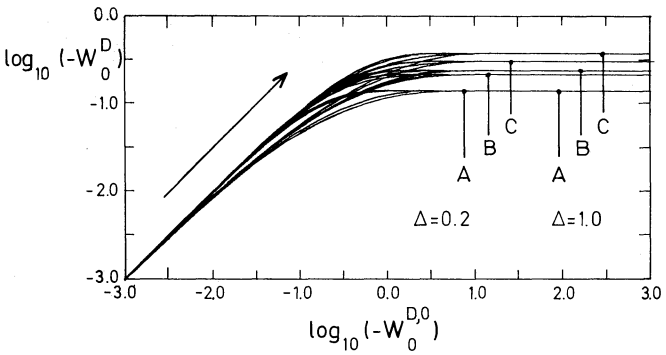

Fig. 6. "$\log_{10}(-W_0^D) - \log_{10}(-W_0^{D,0})$" curves calculated for the eighteen possible models from Table 1. The results are shown for two values of the doublet separation Δ. A, B and C refer to the different velocity fields used for modeling the expanding atmosphere

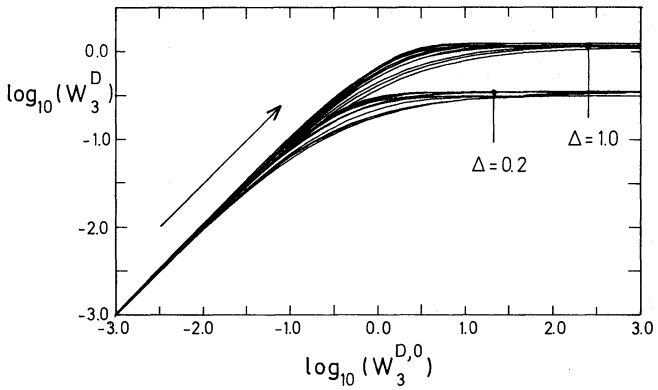

Fig. 7. "$\log_{10}(W_3^D) - \log_{10}(W_3^{D,0})$" curves calculated for the eighteen possible models from Table 1 and two different doublet separations

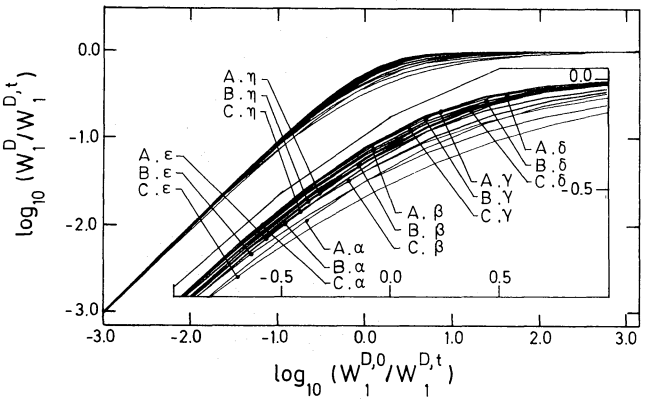

Fig. 9. Same as in Fig. 8 but for "$\log_{10}(W_1^D/W_1^{D,t}) - \log_{10}(W_1^{D,0}/W_1^{D,t})$" curves

One notices immediately that apart from a mere translation (cf. the indicated arrow), there exists a great similarity between two curves pertaining to a same velocity and opacity model but different values of the doublet separation. With the exception of a few notable cases (cf. $n = 2$ and $\Delta \geq 0.6$; $n = 3$ and $\Delta \geq 1.2$ for the models A.α, A.η, B.η and C.η further described in Hutsemékers and Surdej, 1989a), this trend appears to be very general and we can take advantage of this as follows. Let us construct from our data "$\log_{10}(W_n^D/W_n^{D,t}) - \log_{10}(W_n^{D,0}/W_n^{D,t})$" diagrams (see Figs. 8-11). In agreement with our previous statement, we find that, within a very good approximation, these new diagrams are independent on the value of the doublet separation Δ. It therefore becomes possible, on the basis of a single "$\log_{10}(W_n^D/W_n^{D,t}) - \log_{10}(W_n^{D,0}/W_n^{D,t})$" diagram to determine the value of the parameter $W_n^{D,0}$ from the measurement of W_n^D and the knowledge of $W_n^{D,t}$ versus Δ (cf. Figs. 2-5). If the P Cygni line profile under study is sufficiently unsaturated, our measurements fall on the linear part of the curves and we recover the result $W_n^{D,0} = W_n^D$, irrespective of the velocity and opacity distributions. As the observed line profile gets more saturated, the derived value of $W_n^{D,0}$ becomes more and more dependent on the choice of the velocity and opacity distributions. It is only then possible to derive a lower limit to the value of the parameter $W_n^{D,0}$. As $\log_{10}(W_n^{D,0}) \to \infty$, $\log_{10}(W_n^D)$ tends towards the asymptotic value

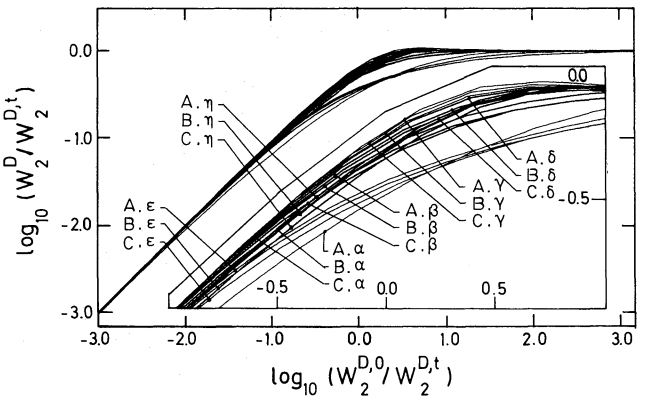

Fig. 10. Same as in Fig. 8 but for "$\log_{10}(W_2^D/W_2^{D,t}) - \log_{10}(W_2^{D,0}/W_2^{D,t})$" curves

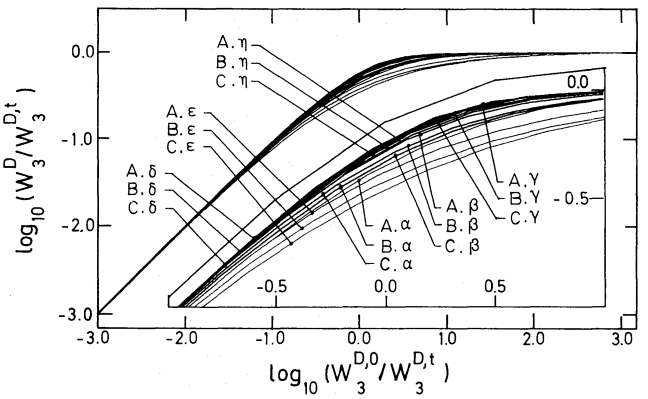

Fig. 11. Same as in Fig. 8 but for "$\log_{10}(W_3^D/W_3^{D,t}) - \log_{10}(W_3^{D,0}/W_3^{D,t})$" curves

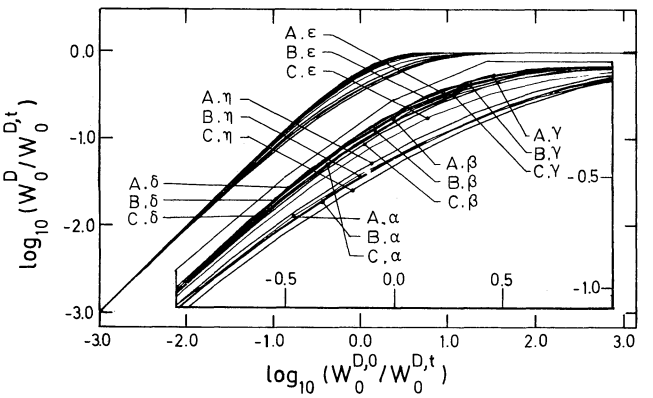

Fig. 8. "$\log_{10}(W_0^D/W_0^{D,t}) - \log_{10}(W_0^{D,0}/W_0^{D,t})$" curves calculated for the eighteen possible models from Table 1 and $\Delta = 0.5$. Note that within a very good approximation, these calculations are irrespective of the doublet separation Δ

$\log_{10}(W_n^{D,t})$ (see Sect 3.4). As already discussed for the case of a single resonance line transition (Surdej, 1985–Paper III–), it should also be very useful to represent in theoretical "$\log_{10}(W_n^D) - \log_{10}(W_{n'}^D)$" or "$\log_{10}(W_n) - \log_{10}(W_{n'}^D)$" diagrams observed values of the corresponding moments in order to infer the type of the velocity and opacity distributions characterizing the line profiles under study. A general look at our data (cf. Figs. 8-11) indicates that for odd values ($n = 1, 3, \ldots$) of the order, the moments are mostly sensitive to the form of $\tau_D^r(X')$ whereas for even values ($n = 0, 2, \ldots$) of n, the moments are opacity dependent at

moderate optical depths but entirely velocity dependent as the line profile gets progressively saturated. Therefore, we suggest as a first possible application to use simultaneously "$\log_{10}(W_1^D) - \log_{10}(-W_0^D)$" and "$\log_{10}(W_3) - \log_{10}(W_1^D)$" diagrams in order to characterize at best the velocity and opacity distributions from measurements of the relevant moments. Such diagrams are illustrated in Figs. 12 and 13 for $\Delta = 0.5$. Note that for optically thin lines, the linear part of the theoretical curves is irrespective of the doublet separation (their slopes may be found in Table 3). It is very likely that other combinations of the calculated moments will prove useful to the interpretation of observed line profiles. Any such diagrams may be constructed from the numerical data compiled in Hutsemékers and Surdej (1990).

6. Physical representation of the parameters $W_n^{D,0}$ and W_n^0

Following a similar approach as in Paper III for the case of a single resonance line transition and adopting the definitions

$$V_n^0 = W_n^{D,0} \quad \text{for } n = 0, 1,$$
$$V_n^0 = W_n^0 \quad \text{for } n = 2, 3, \tag{50}$$

we may combine Eqs. (36), (41), (42) and (49) to derive the interesting relation

$$V_n^0 = K\dot{M}\overline{X'^{n-1}}\bar{n}^{(n)}(\text{level})q^{cn}(\infty)\frac{A(\text{el})}{v_\infty^2}. \tag{51}$$

The average quantities are defined as

$$\overline{X'^{n-1}} = \frac{\int_1^\infty X'^{n-1} n(\text{level}) F_n(L)\, dL}{\int_1^\infty n(\text{level}) F_n(L)\, dL} \tag{52}$$

and

$$\bar{n}^{(n)}(\text{level}) = \frac{\int_1^\infty n(\text{level}) F_n(L)\, dL}{\int_1^\infty F_n(L)\, dL}. \tag{53}$$

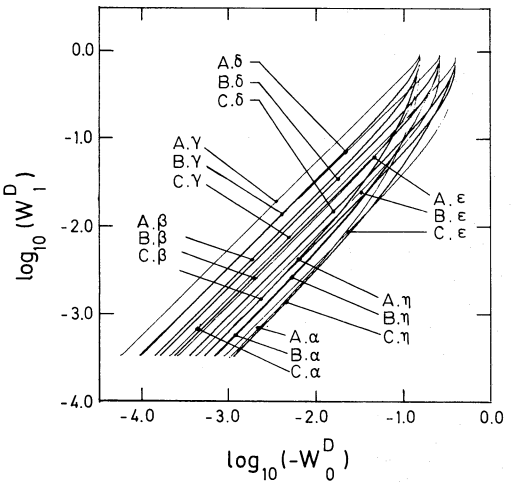

Fig. 12. "$\log_{10}(W_1^D) - \log_{10}(-W_0^D)$" curves calculated for the eighteen possible models from Table 1 and $\Delta = 0.5$. Here, the linear part of the curves remains independent on the doublet separation. However, the saturated part (higher values of $|W_0^D|$ and W_1^D) is very much dependent on Δ

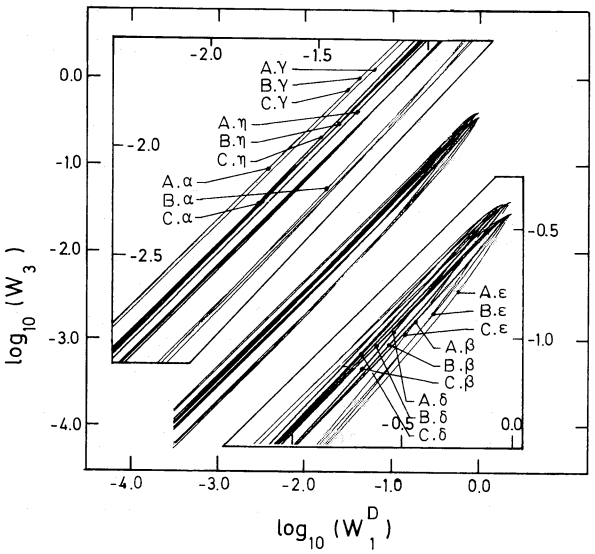

Fig. 13. Same as in Fig. 12 but for "$\log_{10}(W_3) - \log_{10}(W_1^D)$" curves

We also have

$$q^{cn}(\infty) = \int_1^\infty F_n(L)\, dL, \tag{54}$$

where the function $F_n(L)$ is expressed by

$$F_0(L) = \frac{4L^2W - 1}{L^2},$$
$$F_1(L) = -\frac{(1-W)}{L^2},$$
$$F_2(L) = \frac{2}{3}(1 - W(1 + (1-2W)^3) - (1-2W)^3), \tag{55}$$
$$F_3(L) = -\frac{1}{L^2}\left(1 - \frac{1}{2L^2}\right)(1-W),$$

leading to the values $q^{c0}(\infty) = 0.14159$, $q^{c1}(\infty) = -0.89271$, $q^{c2}(\infty) = 0.60971$ and $q^{c3}(\infty) = -0.76029$.

Adopting the following relations

$$Q_n = \frac{V_n^0 v_\infty^{n+1}}{Kq^{cn}(\infty)}, \tag{56}$$

and

$$R_n = -\frac{Q_n q^{cn}(\infty)}{4\pi\bar{\mu}M_{\text{amu}}R_*}, \tag{57}$$

we easily find by means of Eqs. (42) and (51)–(54) that the above expressions reduce to

$$Q_n = \dot{M}\overline{v^{n-1}}\,\bar{n}^n(\text{level})A(\text{el}), \tag{58}$$

and

$$R_n = \int_{R_*}^\infty n_1(r)v(r)^n F_n(L)L^2\, dr, \tag{59}$$

where $n_1(r)$ represents the volume density of the relevant ion in the lower atomic level. As for the case of a single resonance line transition, the above results permit to conclude that for $n = 1, 2$

Table 3. The ratios V_n^0/V_1^0, $\bar{n}^{(n)}(\text{level})/\bar{n}^{(1)}(\text{level})$ and the average quantity $\overline{X'^{n-1}}$ (see Eqs. (50)–(53), $n = 0$, 2 and 3) for the velocity laws (A)–(C) and the opacity distributions (α)–(η) (see Table 1)

	n	(A)			(B)			(C)		
		V_n^0/V_1^0	$\bar{n}^{(n)}/\bar{n}^{(1)}$	$\overline{X'^{n-1}}$	V_n^0/V_1^0	$\bar{n}^{(n)}/\bar{n}^{(1)}$	$\overline{X'^{n-1}}$	V_n^0/V_1^0	$\bar{n}^{(n)}/\bar{n}^{(1)}$	$\overline{X'^{n-1}}$
(α)	0	3.2590	1.0000	20.523	2.1763	1.0000	13.705	0.6419	1.0000	4.0426
	2	0.2461	1.0000	0.3599	0.3641	1.0000	0.5325	0.4729	1.0000	0.6917
	3	0.1792	1.0000	0.2104	0.3483	1.0000	0.4090	0.4917	1.0000	0.5773
(β)	0	0.4364	0.3291	8.3498	0.7361	0.7662	6.0501	1.5854	1.9861	5.0270
	2	0.3430	0.9890	0.5073	0.3531	1.0024	0.5151	0.3676	1.0117	0.5313
	3	0.3019	1.0942	0.3240	0.2950	1.0069	0.3440	0.2816	0.8805	0.3755
(γ)	0	0.1754	0.1531	7.2116	0.2955	0.3814	4.8785	0.6419	1.0000	4.0426
	2	0.4375	0.9821	0.6514	0.4588	0.9909	0.6772	0.4729	1.0000	0.6917
	3	0.4732	1.1348	0.4896	0.4985	1.0824	0.5408	0.4917	1.0000	0.5773
(δ)	0	0.2926	0.2366	7.7860	0.5009	0.5766	5.4712	1.0840	1.5041	4.5388
	2	0.3862	0.9855	0.5731	0.3990	0.9972	0.5850	0.4140	1.0071	0.6011
	3	0.3772	1.1150	0.3972	0.3780	1.0423	0.4258	0.3670	0.9339	0.4614
(ε)	0	0.7847	0.5231	9.4474	1.2767	1.1214	7.1704	2.7207	2.8648	5.9807
	2	0.2793	0.9954	0.4103	0.2874	1.0101	0.4161	0.2992	1.0157	0.4308
	3	0.2023	1.0537	0.2254	0.1923	0.9486	0.2380	0.1775	0.8022	0.2598
(η)	0	1.6787	0.5660	18.678	2.1763	1.0000	13.705	3.6976	2.2554	10.325
	2	0.3441	0.9908	0.5079	0.3641	1.0000	0.5325	0.3815	1.0042	0.5556
	3	0.3299	1.0691	0.3623	0.3483	1.0000	0.4090	0.3476	0.9013	0.4528

and 3, Q_n represents the mass-loss rate, an average momentum rate and (twice) an average kinetic energy rate carried out by the relevant species in the flow. Except for $n = 0$, the dependence of the average fractional abundance $\bar{n}^{(n)}$ (level) as a function of the order n is quite small (see Table 3). It is interesting to compare at this stage the values V_n^0/V_1^0, $\bar{n}^{(n)}/\bar{n}^{(1)}$ and $\overline{X'^{n-1}}$ reported in Table 3 with those derived for the case of a single resonance line transition (cf. Table 2 in Paper III). The similarities and differences existing between those quantities are easily understood on account of the basic definitions and properties of the respective moments. Another interpretation of the physical parameter V_n^0 may be obtained from Eq. (59). Indeed, for $n = 1, 2$, etc. the quantity R_n provides a measure of the column velocity, (two third of) the column square velocity, etc., of the species under consideration. For $n = 0$, we obtain

$$R_0 = \int_{R_*}^{\infty} n_1(r)(4L^2W - 1)\,dr\,, \tag{60}$$

and since $4L^2W \simeq 1$, this quantity ceases to provide an estimate of the column density. This result constitutes a major difference with that obtained for the case of a single resonance line transition (cf. Paper III). The necessity to adopt different definitions for the moments W_n^D and W_n^s (see Introduction) is the main cause of this.

7. Conclusions

Because most of the P Cygni profiles observed in the ultraviolet spectra of early-type stars, planetary nebula nuclei and in the optical spectra of high redshift BAL quasars are due to lines such as C IV $\lambda\lambda$ 1548.2, 1550.8, Si IV $\lambda\lambda$ 1393.8, 1402.8, N V $\lambda\lambda$ 1238.8, 1242.8, O VI $\lambda\lambda$ 1031.9, 1037.6, etc., for which $\Delta v_{23} = 498$, 1939, 965, 1653 km/s, respectively, there is a real need to develop the theory of the n^{th} order moment W_n^D for the particular case of a *resonance doublet transition*. The present work merely constitutes a first step in that direction and we therefore discuss at the end of this section the limits of the applicability of our method to real sets of observations.

But first of all, let us summarize the content of this contribution to the theory of the n^{th} order moment W_n^D: deriving a suitable expression for the resonance doublet profile $E(X_D)/E_c$ (see Eq. (15)), we have established the general expression of the moment W_n^D in Eq.(33). We have demonstrated that, in the optically thin case, the latter equation reduces to the same expression as that directly obtained for a resonance doublet approximated by two independent line transitions. This same result applies in the optically thick approximation provided that the doublet separation $\Delta \geq 2$. For $\Delta < 2$, the asymptotic value $W_n^{D,t}$ remains very dependent on Δ as well as on the type of the velocity field $v(r)$ (see Figs. 2-5).

Adopting realistic expressions for $v(r)$ and for the opacity distribution $\tau_D^r(X')$, we have performed extensive calculations of W_n^D ($n = 0, 1, 2$ and 3). A few diagrams of astrophysical interest have been presented. We have namely discussed the potential use of the normalized "$\log_{10}(W_n^D/W_n^{D,t}) - \log_{10}(W_n^{D,0}/W_n^{D,t})$" diagrams in order to infer the values of the parameters $W_n^{D,0}$ (see Figs. 8–11). For unsaturated P Cygni line profiles, we recover (cf. Paper III) the very useful relation $W_n^{D,0} = W_n^D$, irrespective of the choice of $v(r)$, $\tau_D^r(X')$ and of the doublet separation Δ. We have shown that the physical parameters $W_n^{D,0}$ (and simple linear

combinations of these) are simply related to quantities of astrophysical interest. For $n = 1, 2$ and 3, the above parameters are directly expressed in terms of the mass-loss rate, an average impulsion rate and (twice) an average kinetic energy rate, respectively, carried out by the relevant species in the expanding atmosphere. We have also suggested to use simultaneously the "$\log_{10}(W_1^D) - \log_{10}(-W_0^D)$" and "$\log_{10}(W_3) - \log_{10}(W_1^D)$" diagrams in order to determine the types of $v(r)$ and $\tau_D^r(X')$.

As far as the applicability of the present method is concerned, let us stress here that we did not include yet in the theory the possible departures from the Sobolev approximation (cf. the "turbulence" effects discussed by Bertout, 1984 and Lamers et al., 1987), the effects of underlying photospheric absorption lines for the resonance doublet transitions (but see Surdej, 1982 for a discussion of this effect on the first order moment W_1^s). Furthermore, if "shell components" are seen to perturb the observed absorption trough, they should be taken away before measuring the moments of the intrinsic P Cygni profiles. Potential users of the theory of the moments W_n^D should therefore be aware of the above limitations before applying it to real observations (cf. IUE spectra of O-type stars). We personnally consider that the "moments" method should allow one to test efficiently the theory against observations, in a statistical sense. For instance, comparison between theoretical and observed "$\log_{10}(W_n^D) - \log_{10}(W_{n'}^D)$" diagrams constructed from a large sample of P Cygni profiles should help in pointing out the existence of systematic departures and in identifying the physical cause(s). We are presently following such an approach in our analysis of the P Cygni profiles observed in the spectra of high redshift BAL QSOs as well as those displayed in the IUE Atlas of O-type spectra published by Walborn et al. (1985). From the analysis of the latter profiles, we have found out that in addition to the known photospheric and interstellar contamination due to the resonance doublet line transitions, a photospheric pollution of the stellar continuum by several tens of other line transitions is severely affecting each of the different Si IV, C IV, He II and N IV P Cygni profiles (Nemry et al., 1990). As to the improvements to be brought to the model discussed in this paper, we are presently investigating the effects of turbulence (cf. Lamers et al., 1987) onto "$\log_{10}(W_n^D) - \log_{10}(W_n^{D,0})$" and "$\log_{10}(W_n^D) - \log_{10}(W_{n'}^D)$" diagrams similar to those illustrated in Figs. 5-13. Of course, no difference should be found for the most interesting case of unsaturated, resonance doublet, P Cygni profiles.

Let us still finally mention that since the theory of the moments W_n^D is particularly well suited to the interpretation of under-resolved line profiles (see Castor et al., 1981), P Cygni profiles observed with IUE in the low resolution mode provide us with a potential set of observations to be analysed in this way. As a first application of the present results, Hutsemékers and Surdej (1989) have revisited the mass-loss rates of seventeen central stars of planetary nebulae observed with IUE.

Acknowledgements. It is a great pleasure to thank Véronique Hutsemékers for her help in typing the manuscript and Armand Kransvelt for drawing the figures.

Appendix A

By means of Eq. (II.70), i.e. Equation (70) in Paper II, we easily establish that the expression for the moment $W_n^{ij}(n = 0, 1, 2$ and 3) of a single resonance line transition $i \rightleftharpoons j$ reduces to

$$W_0^{ij} = \int_{-X_{\min}}^{1} \tau_{ij}^r(X')(1 - 4L^2 W)\, dX',$$

$$W_1^{ij} = \int_{-X_{\min}}^{1} X' \tau_{ij}^r(X')(1 - W)\, dX', \tag{A.1}$$

$$W_2^{ij} = \int_{-X_{\min}}^{1} X'^2 \tau_{ij}^r(X') \frac{2}{3}(W(1 + (1 - 2W)^3) - 1 + (1 - 2W)^3)L^2\, dX',$$

$$W_3^{ij} = \int_{-X_{\min}}^{1} X'^3 \tau_{ij}^r(X') \left(1 - \frac{1}{2L^2}\right)(1 - W)\, dX'.$$

Since the fictitious radial opacity τ_{ij}^r is proportional to the oscillator strength f_{ij} (see Eq. (II.19)), we also have $W_n^{ij} \propto f_{ij}$.

Appendix B

Inserting expression (16) for $E_{12}(X)/E_c$ into Eq. (5) for the moment W_n^D leads to the result

$$W_n^{D,12} = \int_{-1+\varepsilon\Delta}^{\varepsilon\Delta} X_D^n \int_{\max(|X_D - \varepsilon\Delta|, -X_{\min})}^{1} \cdot P_{12}^N(X')\, P_{12}(X', X_D - \varepsilon\Delta) \frac{dX'}{2X'}\, dX_D + \int_{\varepsilon\Delta}^{X^0 + \varepsilon\Delta} X_D^n \int_{\max(|X^N|, -X_{\min})}^{1} \cdot P_{12}^N(X')\, P_{12}(X', X_D - \varepsilon\Delta) \frac{dX'}{2X'}\, dX_D. \tag{B.1}$$

We have sketched in Fig. B1 the domain of integration defined by the above sets of integrals in the plane (X_D, X'). Interchanging the order of integration between X_D and X' in the last equation, we find

$$W_n^{D,12} = \int_{-X_{\min}}^{1} \frac{P_{12}^N(X')\, dX'}{2X'} \int_{\varepsilon\Delta - X'}^{X'(1 - 2W(L(X'))) + \varepsilon\Delta} \cdot P_{12}(X', X_D - \varepsilon\Delta)\, X_D^n\, dX_D. \tag{B.2}$$

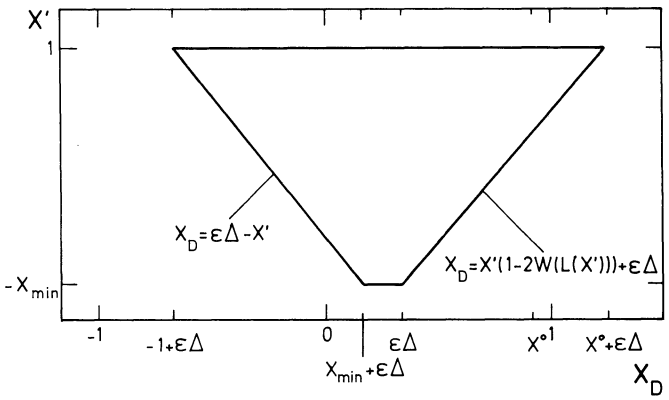

Fig. B1. Domain of integration in the plane (X_D, X') of the integrand $X_D^n P_{12}^N(X')\, P_{12}(X', X_D - \varepsilon\Delta)/2X'$ appearing in Eq. (B.1)

Applying the variable transformation (cf. Eqs. (6) and (24))

$$X_D = -X'\mu + \varepsilon\Delta\,,$$
$$dX_D = -X'd\mu\,, \tag{B.3}$$

and with the help of expressions (22) and (23), we obtain the desired expression for $W_n^{D,12}$ (cf. Eq. (33))

$$W_n^{D,12} = \int_{-X_{\min}}^{1} \frac{\tau_{12}^r(X')(\beta_{12}^5(X') + J_{12}^2(X')/I_c)4L^2(X')}{\beta_{12}^1(X')} \cdot \frac{1}{2} \int_{-(1-2W(L(X')))}^{1} (-X'\mu + \varepsilon\Delta)^n \cdot \frac{(1-\exp(-\tau_{12}(X',\mu)))}{\tau_{12}(X',\mu)}\, d\mu\, dX'\,. \tag{B.4}$$

Appendix C

Under the assumption that the expanding atmosphere is optically thin to the spectral line radiation in the transitions $1 \rightleftharpoons 2$ and $1 \rightleftharpoons 3$, the following approximations:

$$\begin{aligned} \beta_{12}^5(X') &\simeq W\,,\\ \beta_{12}^1(X') &\simeq 1\,,\\ J_{12}^2(X') &\simeq 0\,,\\ \frac{(1-\exp(-\tau_{12}(X',\mu))}{\tau_{12}(X',\mu)} &\simeq 1\,,\\ \frac{(1-\exp(-\tau_{13}(X',\mu))}{\tau_{13}(X',\mu)} &\simeq 1\,,\\ \beta_{13}^3(X') &\simeq W\,,\\ \beta_{13}^1(X') &\simeq 1\,,\\ \exp(-\tau_{12}') &\simeq 1\,, \end{aligned} \tag{C.1}$$

can be conveniently used in the two first sets of integrals of Eq. (33). By means of the variable transformations (6), (7) and (31), (32) and since for constant values of μ_* we have the relations

$$dX = -\frac{\tau_{12}^r(X')}{\tau_{12}(X',\mu_{12})}\frac{dX'}{\mu_{12}}\,,$$
$$dY = -\frac{\tau_{13}^r(Y')}{\tau_{13}(X',\mu_{13})}\frac{dY'}{\mu_{13}}\,, \tag{C.2}$$

we obtain the third set of integrals in Eq. (33)

$$\begin{aligned} &2\int_0^1 \mu_*\, d\mu_* \int_{-\sqrt{1-(1-\mu_*^2)/L_{\max}^2}-(1-\varepsilon)\Delta}^{X_{\min}\mu_*+\varepsilon\Delta} X_D^n \cdot (\exp(-\tau_{12}(X',\mu_{12}))\exp(-\tau_{13}(Y',\mu_{13})) - 1)\, dX_D\\ &= -2\int_0^1 \mu_*\, d\mu_* \left[\int_{-X_{\min}}^{1} (-X'\mu + \varepsilon\Delta)^n \tau_{12}^r(X')\frac{dX'}{\mu} + \int_{-X_{\min}}^{1} (-Y'\mu - (1-\varepsilon)\Delta)^n \tau_{13}^r(Y')\frac{dY'}{\mu}\right]. \end{aligned} \tag{C.3}$$

Interchanging the order of integration between μ_* and X', and μ_* and Y' and using afterwards the variable transformation

$$\mu = \sqrt{1-(1-\mu_*^2)/L^2}\,,$$
$$\mu\, d\mu = \mu_* d\mu_*/L^2\,, \tag{C.4}$$

the right member of Eq. (C.3) is easily reduced to the result given in Eq. (35).

References

Bertout, C.: 1984, *Astrophys. J.* **285**, 269

Castor, J.I., Lutz, J.H., Seaton, M.J.: 1981, *Monthly Notices Roy. Astron. Soc.* **194**, 547

Hutsemékers, D., Surdej, J.: 1987, *Astron. Astrophys.* **173**, 101

Hutsemékers, D.: 1988, Ph. D. Thesis, University of Liège (Belgium)

Hutsemékers, D., Surdej, J.: 1990 (in preparation)

Hutsemékers, D., Surdej, J.: 1989, *Astron. Astrophys.* **219**, 237

Lamers, H.J.G.L.M., Cerruti-Sola, M., Perinotto, M.: 1987, *Astrophys. J.* **314**, 726

Nemry, F., Surdej, J., Hernaiz, H.: 1990 (in preparation)

Surdej, J.: 1980, *Astrophys. Space Sci.* **73**, 101 (Paper I)

Surdej, J.: 1982, *Astrophys. Space Sci.* **88**, 31 (Paper II)

Surdej, J.: 1983a, *Astrophys. Space Sci.* **90**, 299

Surdej, J.: 1983b, *Astron. Astrophys.* **127**, 304

Surdej, J.: 1985, *Astron. Astrophys.* **152**, 361 (Paper III)

Walborn, N.R., Nichols-Bohlin, J.N., Panek, R.J.: 1985, Nasa Reference Publication 1155